AGU PUBLICATIONS

Geophysical Research Letters

RESEARCH LETTER
10.1002/2014GL062741

Key Points:
- Internal climate variability explains North Atlantic decadal cold events
- Cold events are triggered by weakening of subpolar gyre, not of AMOC
- Related deteriorated conditions contribute to end Greenland Norse settlements

Supporting Information:
- Text S1 and Figures S1–S5

Correspondence to:
E. Moreno-Chamarro,
eduardo.chamarro@mpimet.mpg.de

Citation:
Moreno-Chamarro, E., D. Zanchettin, K. Lohmann, and J. H. Jungclaus (2015), Internally generated decadal cold events in the northern North Atlantic and their possible implications for the demise of the Norse settlements in Greenland, *Geophys. Res. Lett.*, *42*, 908–915, doi:10.1002/2014GL062741.

Received 5 DEC 2014
Accepted 15 JAN 2015
Accepted article online 23 JAN 2015
Published online 13 FEB 2015

Internally generated decadal cold events in the northern North Atlantic and their possible implications for the demise of the Norse settlements in Greenland

Eduardo Moreno-Chamarro[1,2], Davide Zanchettin[1], Katja Lohmann[1], and Johann H. Jungclaus[1]

[1]Max Planck Institute for Meteorology, Hamburg, Germany, [2]International Max Planck Research School on Earth System Modelling, Hamburg, Germany

Abstract We attribute and describe the governing mechanisms of decadal cold excursions in the subpolar North Atlantic of similar amplitude and duration to cold events reconstructed from climate-proxies during the last millennium detected in an ensemble of three transient and one unperturbed climate simulation. The cold events are attributed to internal regional climate variability, with varying external forcing increasing their magnitude and frequency. The underlying general mechanism consists of a feedback loop initiated by a weakening of the North Atlantic subpolar gyre, which induces persistent colder and fresher surface conditions in the Labrador Sea and, eventually, a deep convection shutdown. We thus exclude a hemispheric climate reorganization or a weak ocean overturning circulation as necessary trigger for such events. An associated northeastward atmospheric cold advection over the Labrador Sea deteriorates local living conditions on south Greenland, essential for the sustainability of the Norse settlements.

1. Introduction

The Norse expansion to Iceland, Greenland, and, eventually, North America was likely favored by the mild climate conditions over the Northern Hemisphere by the beginning of the last millennium, in the so-called Medieval Climate Anomaly [*Ogilvie et al.*, 2000; *Kuijpers et al.*, 2014]. The loss of their Greenland settlements some centuries later, in contrast, roughly coincides with the onset of the Little Ice Age [*Ogilvie et al.*, 2000; *Kuijpers et al.*, 2014], the anomalously cold period spanning the fourteenth to the nineteenth century. Worsening local living conditions associated with a colder Northern Hemisphere climate might thus have contributed, in combination with other factors, to this demise [*Dugmore et al.*, 2012]. Since relevant aspects of such local environmental change remain unclear, this study aims at investigating whether it was necessarily caused by external forcing, as well as whether regional rather than global processes were determinant.

Climate variability over southern Greenland is largely influenced by that of the northern North Atlantic sector [e.g., *Kuijpers et al.*, 2014], which in turn is shaped by different modes of atmospheric and oceanic variability, such as the North Atlantic Oscillation (NAO), or the Atlantic Meridional Overturning Circulation (AMOC) [e.g., *Marshall et al.*, 2001; *Grossmann and Klotzbach*, 2009]. Over the last years, attention has focused on better understanding the dynamics of the surface circulation in the subpolar North Atlantic, namely the subpolar gyre [e.g., *Langehaug et al.*, 2012; *Born and Stocker*, 2014]. This basin-wide cyclonic oceanic gyre is primarily driven by wind forcing and buoyancy differences within the subpolar North Atlantic between 50°N and 65°N [e.g., *Marshall et al.*, 2001]. It transports warm and saline tropical water northward and cold and fresh polar waters southward along its eastern and western rims, respectively. The subpolar gyre is furthermore an important component of the thermohaline circulation [*Hátún et al.*, 2005]: variations in the gyre's strength can modulate the salt transport to the Labrador Sea and the Nordic Seas, where oceanic deep mixing takes places. Thus, the subpolar gyre has been described as a relevant driver of the climate variability of the North Atlantic on different time scales [e.g., *Moffa-Sánchez et al.*, 2014a; *Jungclaus et al.*, 2014].

Climate reconstructions along the coasts of Iceland and southern Greenland show prominent interdecadal cold events before the Norse settlement demise [e.g., *Patterson et al.*, 2010; *Moffa-Sánchez et al.*, 2014b]. These reconstructions associate cold events with increased transport of cold and ice-rich polar waters by the East Greenland Current from the Arctic Ocean to the subpolar North Atlantic [e.g., *Ran et al.,* 2011; *Moffa-Sánchez et al.,* 2014b], as well as with weaker advection of warm tropical waters by the subpolar gyre [*Moffa-Sánchez et al.,* 2014a]. Additionally, these changes are somehow linked to long-term fluctuations in

the large-scale atmospheric circulation, like those described by the NAO [see *Patterson et al.*, 2010; *Kuijpers et al.*, 2014], or atmospheric blocking situations [*Moffa-Sánchez et al.*, 2014a]. The intrusion of relatively fresh waters into the Labrador Sea could have also reduced deep water formation and, thereby, weakened the AMOC and the associated northward heat transport [e.g., *Miller et al.*, 2012].

It is uncertain whether the cold events occurred as an externally forced response, i.e., as a consequence of variations of the Earth's energy budget forced by external agents (e.g., volcanic eruptions), or due to internal climate variability, i.e., from spontaneous dynamics and feedbacks within the climate system [e.g., *Hasselmann*, 1976]. Similar timing has been found between proxy-based temperature reconstructions and frequency and magnitude of solar minima [*Ran et al.*, 2011; *Moffa-Sánchez et al.*, 2014a] and a cluster of explosive volcanic eruptions [*Sicre et al.*, 2011; *Miller et al.*, 2012]. Last millennium climate simulations support both the solar [e.g., *Jiang et al.*, 2005; *Moffa-Sánchez et al.*, 2014a] and the volcanic hypothesis [e.g., *Sicre et al.*, 2011]. However, major cold excursions in the paleorecords also occur during periods characterized by weak external forcing [e.g., *Sicre et al.*, 2011], pointing to a nonnegligible role of internal climate variability.

Accordingly, a realistic shift from a warm to a cold period over the Norse Greenland settlements spontaneously emerges in a multimillennial unperturbed control climate simulation [*Hunt*, 2009]. The onset and persistence of the cold regime is attributed to stochastic influences, excluding large-scale modes of atmospheric variability, like the NAO, as possible drivers [*Hunt*, 2009].

In view of these partly contradictory results, this study investigates the dynamics underlying decadal-scale cold events in the northern North Atlantic detected in an ensemble of three last millennium transient coupled climate simulations and in the associated unperturbed control experiment, thus complementing contributions from previous studies. We aim to answer the following questions: What are the mechanisms behind these cold events and are they similar for all the cold events considered? Are such events only triggered by external forcing, or are they part of the internal climate variability? Are they necessarily linked to large-scale phenomena or hemispheric/global climate variability?

2. Model Description and Experimental Setup

The simulations were performed with the Max Planck Institute for Meteorology Earth System Model for paleo-applications (MPI-ESM-P). The atmosphere general circulation model European Centre/Hamburg 6 (ECHAM6) [*Stevens et al.*, 2013] is run at horizontal resolution T63 (1.875° × 1.875°) and 47 vertical levels, resolving the stratosphere up to 0.01 hPa. The ocean-sea ice model Max Planck Institute Ocean Model (MPIOM) [*Jungclaus et al.*, 2013, and references therein] applies a conformal mapping grid in the horizontal with the North Pole over southern Greenland featuring a nominal resolution of 1.5°. The convergence of the mesh size toward the poles translates into a grid spacing of 15 to 100 km in the North Atlantic, providing a relatively high resolution in the study area (i.e., deep water formation regions in the Northern Hemisphere). Vertically, 40 unevenly spaced z levels are used with the first 20 levels covering the upper 700 m of water column.

We use three last millennium all-forcing transient simulations between 850 and 1849 (hereafter Past1000–R1, Past1000–R2, and Past1000–R3) following the CMIP5/Paleoclimate Modelling Intercomparison Project 3 (PMIP3) protocol [*Schmidt et al.*, 2011; *Braconnot et al.*, 2012]. Prescribed external forcing factors are as follows: reconstructed variations in volcanic aerosols [*Crowley and Unterman*, 2012], total solar irradiance (TSI) [*Vieira et al.*, 2011], atmospheric concentration of most important well-mixed greenhouse gases and anthropogenic aerosols, land cover changes [*Pongratz et al.*, 2008], and changes in orbital parameters. Additionally, we use a control run under constant preindustrial (1850) boundary conditions (hereafter PiControl) as required by the CMIP5/PMIP3 protocol. The integration of the Past1000 simulations is started after a 400 year spin-up from the PiControl's last integration year and with constant 850 boundary conditions. Further information on these runs, the experimental setup, and the model is provided by *Jungclaus et al.* [2014].

3. Methods

Proxy-based reconstructions of changes in seawater properties over the Eirik Drift have been recently used to investigate the northern North Atlantic climate variability during the last millennium [*Moffa-Sánchez et al.*, 2014b, H. F. Kleiven et al., personal communication, 2014]. This location, at about 60°N and 55°W to the south of

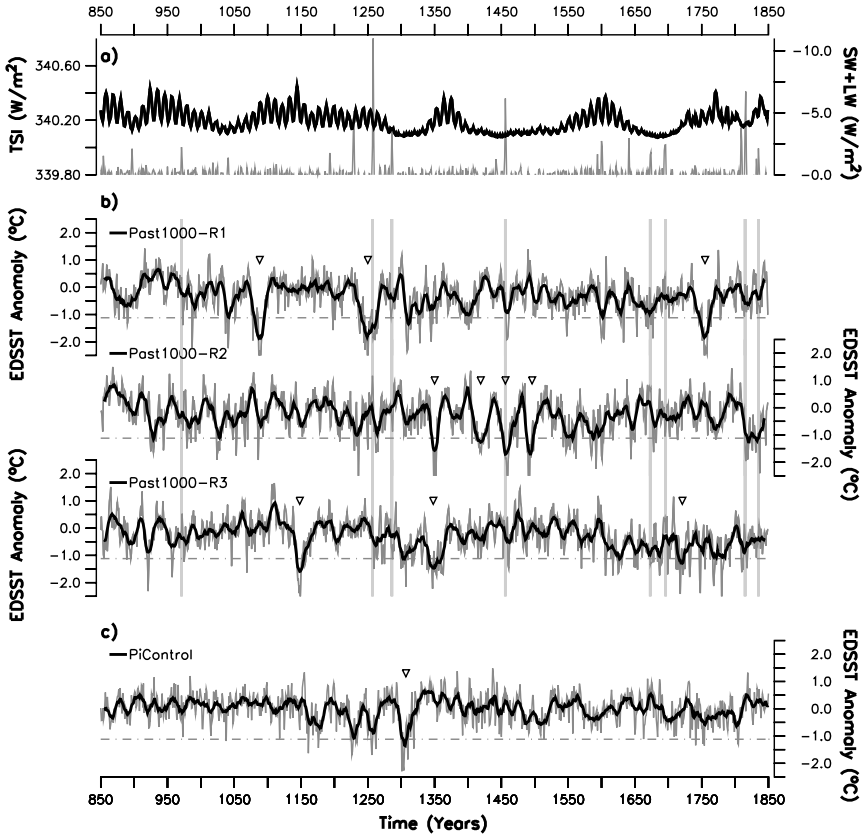

Figure 1. (a) Annual globally averaged values of the reconstructed TSI (black line, in W/m^2) [*Vieira et al.,* 2011], and of the simulated volcanic forcing shown as net radiative flux anomalies, i.e., long plus short waves (LW + SW, in W/m^2), at the top of the atmosphere with respect to the climatological mean. The shown volcanic forcing is for Past1000-R1. Timing of volcanic eruptions is the same in all Past1000s, as they are all based on the reconstructed aerosol properties by *Crowley and Unterman* [2012], but the magnitude of the forcing slightly differs [see *Jungclaus et al.*, 2014]. (b and c) Annual SST anomalies (in °C; grey line) averaged over the Eirik Drift (55°N–60°N and 40°W–50°W, black box in Figure 2a) in the Past1000s and PiControl, respectively. Anomalies are calculated with respect to the PiControl climatological mean. Black lines are the 11 year running mean. Horizontal dash-dotted lines account for the −1.1°C threshold (see text), and triangles outline the cold events that satisfy this criterion. Vertical lines in Figure 1b represent an ensemble of strong volcanic eruptions considered by *Zanchettin et al.* [2012].

Greenland (black box in Figure 2a), is well situated to monitor and estimate surface and subsurface variations in both the East Greenland Current and the Irminger Current, which constitute the northern rim of the subpolar gyre.

Decadal-scale cold periods in the northern North Atlantic are detected based on smoothed (11 year running mean) annual sea surface temperature (SST) anomalies at the Eirik Drift site (hereafter EDSST anomalies). These are calculated for each simulation with respect to the PiControl climatological mean, which provides estimates of the simulated internal climate variability. To focus on decadal-scale events, we only consider periods with sustained EDSST anomalies below −1.1°C during five or more consecutive years. This threshold value (Figures 1b and 1c, horizontal dash-dotted lines) corresponds to the 5th percentile of the distribution of the combined Past1000 EDSST anomalies. This criterion therefore incorporates information about both the relative frequency and the magnitude of clustered cold years, without further discrimination of the two contributions. Our results for the detected cold events do not appreciably change if a different criterion is applied (e.g., with respect to the distribution of EDSST anomalies in PiControl). Long-lasting cold events are also expected to have a more significant impact on the Norse society in Greenland [*Dugmore et al.*, 2012].

Dynamical interpretation of the cold events is based on analysis of the associated composite of anomalies from the unperturbed climatology. The coldest year of each event (hereafter year-0) is used as reference for the compositing. Statistical significance is estimated based on the likelihood of a random occurrence of the signal in PiControl, i.e., we assess their attribution to internal variability alone. Specifically, the signal obtained for

the selected cold events in the Past1000s is compared to that obtained from randomly sampling 500 times the same number of events from the full period of PiControl, treating these random events in the same way as actual cold events. Percentile intervals of the empirical anomaly distribution obtained from the randomization are used to determine the confidence levels associated with a random occurrence of the signal.

4. Results

We identify 10 cold events in the three Past1000s (triangles in Figure 1b), according to our criterion. These events show negative EDSST anomalies lasting for about 20–40 years, with the coldest anomalies ranging between −1.5°C and −2°C. Simulated cold events are thus of similar amplitude and duration to those reconstructed within the northern North Atlantic during the last millennium [e.g., *Sicre et al.*, 2011; *Moffa-Sánchez et al.*, 2014b]. The cold events appear scattered throughout the Past1000s and events of different experiments do no robustly overlap in time. Besides, these can develop isolated in time (e.g., around 1090 in Past1000-R1) or in series of events (e.g., after 1400 in Past1000-R2). One cold event of similar characteristics, i.e., duration and amplitude, as in the Past1000s is identified in PiControl (Figure 1c). The smaller amplitude of EDSST variability in PiControl compared to that in the Past1000s suggests an influence from external forcing. However, cold events in the Past1000s are generally found outside periods characterized by anomalous external forcing, such as solar minima (Figure 1a), or major volcanic eruptions (Figure 1a and vertical bars in Figure 1b). Only a few cold events occur after a major volcanic eruption, and the response of the EDSSTs is never robust across the three simulations, as exemplified by the 1228 event, which is associated to a strong cold excursion in Past1000-R1, and a slight warming in R3. Furthermore, EDSSTs are not robustly lag-correlated with the TSI and the volcanic forcing (Figures S1a and S1b in the supporting information, respectively), and the North Atlantic response to volcanic forcing (Figure S2 in the supporting information) differs from the evolution around the cold events described below. The slightly negative trend in the EDSST time series could partly be attributed to varying orbital parameters [*Kaufman et al.*, 2009]. However, the detected cold events do not cluster at either side of the simulation; rather, they occur throughout the integration time, suggesting a negligible role of millennial-scale changes in the background state. So, we conclude that such events can be triggered by internal climate variability alone. External forcing, nevertheless, appears to be indirectly involved though a general amplification of EDSST variability under forced conditions, favoring the development of more frequent deeper cold events. This might be related to a colder climate background state in the forced runs. Understanding the role of external forcing on the general climate state is, however, beyond the scope of our study.

In the following, composite anomalies of the 10 cold events detected in the Past1000s (triangles in Figure 1b) describe their underlying mechanism and their imprint on the North Atlantic climate. Figure 2 illustrates the North Atlantic climate anomalies associated with this composite, and Figure 3 shows the temporal evolution around year-0 of composite standardized indices of climatic quantities. For the sake of clarity, we only show a single interval of significance between ±1.07 in Figure 3, corresponding to the largest nonsignificant anomaly among all depicted variables. Therefore, anomalies exceeding this interval are always significant.

The cold events are characterized by a broad cooling of the subpolar North Atlantic surface (Figure 2a), more intense to the west of the oceanic basin, with the coldest anomalies found in the Labrador Sea and along the southern coast of Greenland. A similar pattern characterizes sea surface salinity (SSS) anomalies in this region (Figure 2b), with a widespread surface freshening in the northwestern North Atlantic. This cooling and freshening of the upper northern North Atlantic becomes significant over the Eirik Drift about 11 years before the peak of the event (Figure 3). More generally, simulated EDSST and Eirik Drift SSS (hereafter EDSSS) changes on decadal and longer time scales are very highly correlated ($r \sim 0.8$; $p < 0.05$) throughout the entire millennium in all the Past1000s (not shown). Within the northern North Atlantic, freshening when cooling, and vice versa, is also described by marine proxy-based reconstructions for the last millennium [*Moffa-Sánchez et al.*, 2014b, H. F. Kleiven et al., personal communication, 2014] and by recent direct measurements [*Yashayaev*, 2007].

The anomalous pattern in oceanic surface properties during the cold events (Figures 2a and 2b) is mainly explained by a northwestward shrinking of the subpolar gyre (Figure 2c, shading). In its climatological mean (Figure 2c, contours), the northern branch of the subpolar gyre transports relatively warm and saline water from the North Atlantic Current westward to the Labrador Sea via the Irminger Current. Indeed, the progressive shrinking of the subpolar gyre, which becomes significant about 11 years before the peak of the event (Figure 3), corresponds to progressively colder and fresher surface conditions in the western subpolar

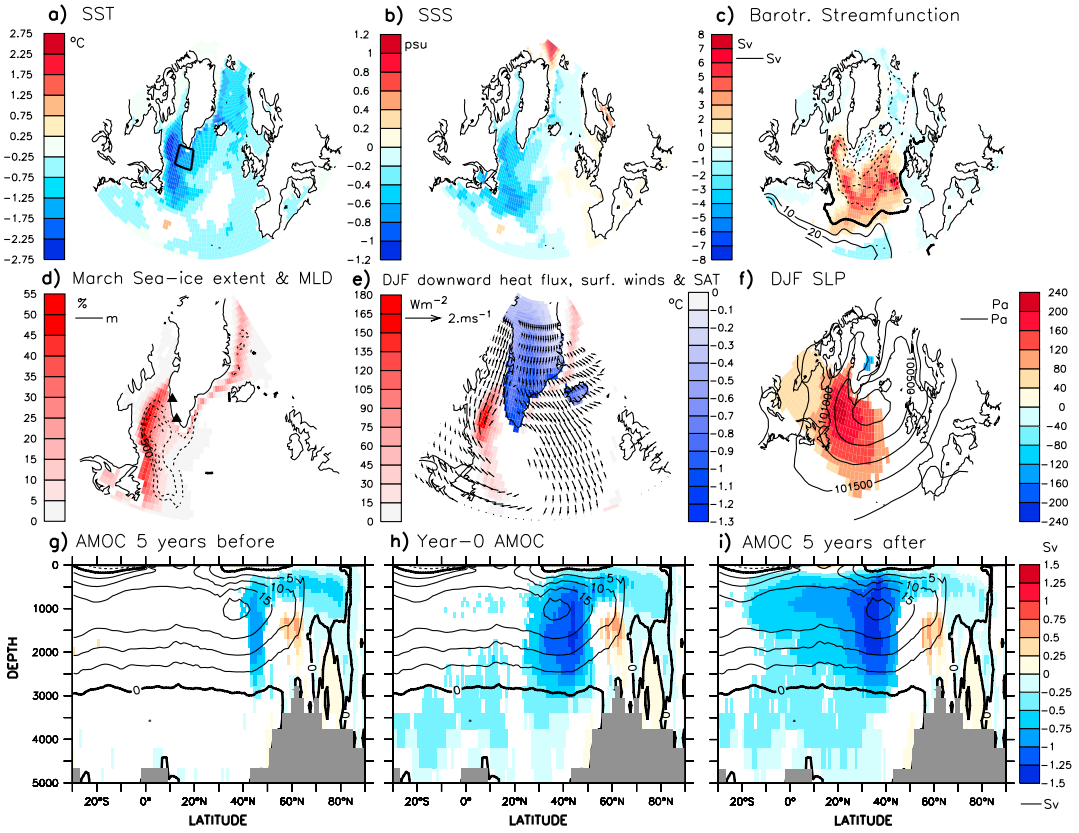

Figure 2. Anomalies for the composite of 10 cold events selected from the Past1000s (triangles in Figure 1b) of (a) SST (in °C), (b) SSS (in practical salinity units (psu)), (c) barotropic stream function (in sverdrup (Sv); shading) with contours representing its climatological mean in PiControl at 10 Sv intervals (dashed/solid lines correspond to cyclonic/anticyclonic flow), (d) ocean mixed layer depth (in meter; contours at 500 m intervals), and sea ice extent (in percent of area; shading), both in March, (e) wintertime (December–February, DJF) ocean heat flux into the ocean (in W/m^2; red shading), surface air temperature (SAT, in °C; blue shading) over Greenland, and near-surface wind anomalies (in m/s; arrows), (f) wintertime (DJF) SLP (in Pascal; shading) with contours representing its climatological mean in PiControl at 500 Pa intervals, and of the AMOC (g) 5 years before, (h) during, and (i) 5 years after the coldest year of the cold events (in Sv; shading), with contours representing its climatological mean in PiControl at 5 Sv intervals. Anomalies are calculated with respect to the climatological mean of PiControl, after having been smoothed with an 11 year low-pass running mean filter. Only anomalies above the 99% confidence level are shown. The black box in Figure 2a outlines the area within the Eirik Drift over which SST anomalies in Figure 1 have been averaged. Triangles in Figure 2d indicate the locations of the former Norse settlements in Greenland [*Ogilvie et al.*, 2000].

North Atlantic (Figure 3). These surface oceanic conditions in the western subpolar North Atlantic therefore result from a reduced volume transport within the northern subpolar gyre, which advects less heat and salt westward, and not from the transport of waters with fresher and colder anomalies from the Arctic via the East Greenland Current, as what observed, for instance, during the 20th century Great Salinity Anomaly [*Gelderloos et al.*, 2012]. Other sources of heat or freshwater to the area, as the local surface fluxes (not shown), or the southward freshwater transport through the Denmark Strait from the Arctic Ocean (Figure 3), show no clear contribution to the surface anomalies during the cold events, in contrast to what has been deduced from paleoreconstructions [e.g., *Moffa-Sánchez et al.*, 2014b].

We find that the weakening of the subpolar gyre can be triggered either by a substantial reduced wind-stress curl over the Irminger Current, or by differential density anomalies between the center and the boundary of the subpolar gyre, negative to the west and positive to the east (not shown), as has been also described by previous studies based on models of diverse complexity [e.g., *Langehaug et al.*, 2012; *Born and Stocker*, 2014]. In either case, once the subpolar gyre starts to weaken, the reduced westward advection of salinity incites a density decrease in the upper levels of the western subpolar basin. With ocean convection here largely controlled by surface densities, and the latter mainly by salinity, the relatively lighter surface waters reinforce water column

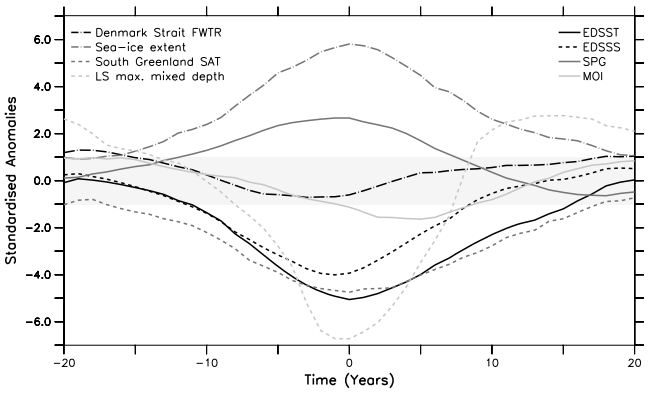

Figure 3. Standardized anomalies of SST and SSS, both averaged over the Eirik Drift (55°N–60°N and 40°W–50°W, black box in Figure 2a), the subpolar gyre (SPG) strength defined as the barotropic stream function averaged between 45°N–70°N and 5°W–60°W, the southward liquid freshwater transport (FWTR) through the Denmark Strait, the sea ice extent averaged between 30°N–90°N and 100°W–0°, the southern Greenland SAT averaged between 60°N–65°N and 40°W–50°W, the Meridional Overturning Index (MOI, defined as the AMOC strength at 1000 m depth and 35°N), and the maximum value of the mixed layer depth in the Labrador Sea (55°N–60°N and 40°W–50°W), during the previous and following 20 years of the composite of the 10 cold events selected from the Past1000s (triangles in Figure 1b). Year 0 corresponds to the coldest year of each cold event. Standardization is done with respect to PiControl after smoothing with an 11 year running mean filter. Light grey shading masks anomalies which are not significant at the 99% confidence level, considering the same range for all variables (see text). Note that subpolar gyre positive/negative anomalies correspond to a weaker/stronger gyre, whereas positive/negative anomalies of the Denmark Strait FWTR represent a saltier/fresher southward flow.

stability and, eventually, shut down late winter convective mixing at the peak of the cold events (Figures 2d, contours, and 3). Colder surface conditions over the Labrador Sea, in turn, reduce the heat flux to the atmosphere and thus the buoyancy flux. This further strengthens water column stratification, contributing to the shutdown of the oceanic deep convection as well [*Gelderloos et al.,* 2012]. The latter reinforces the subpolar gyre weakening by maintaining fresher (hence density negative) anomalies at the surface subpolar basin and, thereby, reducing the density gradient between the gyre's local center and its boundaries [*Born and Stocker*, 2014]. These positive feedbacks dominate the northern North Atlantic climate variability in the initial developing phase of the cold events that lasts about 10–15 years. Then, the induced surface cooling becomes sufficiently strong to compensate the haline-driven surface density decrease in the Labrador Sea. As a result, surface densities progressively increase in the basin center and destabilize the water column, enhancing convective mixing (Figure 3). The latter leads to a strengthening of the subpolar gyre and to larger westward advection of heat and salt. EDSSTs and EDSSSs thus gradually increase toward conditions similar to those before the cold events within about two decades (Figure 3), although with a slower recovery for EDSST than for EDSSS anomalies. This simulated weakening of the subpolar barotropic circulation in the North Atlantic during the cold events is in good agreement with reconstructions of the current speed strength over the Eirik Drift during similar cold periods during the last millennium (H. F. Kleiven et al., personal communication, 2014).

A reduced northward heat transport by a slowed AMOC is often considered as the main trigger of anomalous colder conditions in the North Atlantic [e.g., *Knight et al.*, 2005]. In contrast to the subpolar gyre, the AMOC shows no significant weakening preceding the peak of the cold events (Figures 2g and 3). Instead, the deep water formation shutdown in the Labrador Sea during the cold events forces a progressive and delayed decline of the AMOC (Figures 2h and 3), with the minimum strength typically occurring about 5 years after the coldest year (Figures 2i and 3). An important AMOC weakening can also develop due to anomalous subpolar gyre-driven fresher surface conditions, and not only due to larger freshwater contributions from the Arctic Ocean [e.g., *Miller et al.*, 2012; *Moffa-Sánchez et al.*, 2014b].

The same general mechanism is at play for an ensemble of analogous cold events identified in PiControl determined with a selection criterion based on the distribution of PiControl EDSST anomalies (Figures S3–S5 in the supporting information). The mechanism therefore pertains to the internal variability of the North Atlantic climate.

There are several arguments that support the hypothesis that cold events like those described here could have deeply influenced humans in Greenland. For instance, the anomalously cold surface conditions enhance winter sea ice growth in the western subpolar North Atlantic (Figure 2d, shading) for about 20–30 years (Figure 3). The simulated expanded sea ice agrees well with diatom-based reconstructions [e.g., *Massé et al.*, 2008], and historical records during the end of the Norse colonies in Greenland [*Ogilvie et al.*, 2000]. With the Norse settlements located in the western coast of Greenland (Figure 2d, triangles), the anomalously large sea ice

extent would have conceivably hindered navigation, isolating the fjords where the Norse were settled from the open sea, as well as seal hunting offshore [*Dugmore et al.*, 2012]. Furthermore, increased sea ice cover in the Labrador Sea hampers heat fluxes between the ocean and the atmosphere in the wintertime (Figure 2e, red shading), which results in a large cooling of the overlying air masses.

Anomalously cold surface atmospheric conditions and extended sea ice cover over the Labrador Sea further promote increased atmospheric stability [*Hoskins and Karoly*, 1981], reducing the strength of the low-pressure systems over the North Atlantic during the cold events. The simulated anomalous winter sea level pressure (SLP) pattern consistently entails significant positive anomalies over the western subpolar North Atlantic, and describes a blocking-like structure (Figure 2f, shading), in contrast to studies that associate extremely cold conditions in the Labrador Sea during the instrumental period to positive NAO phases [*Visbeck et al.,* 2003]. Our results are in general agreement with previous model-based results for the last millennium [e.g., *Moffa-Sánchez et al.*, 2014a], although in *Moffa-Sánchez et al.* [2014a] the center of positive pressure anomalies is located further east, over the British Isles.

During the cold events, the anomalous northward atmospheric flow resulting from the SLP anomalies (Figure 2e, arrows) transports relatively cold near-surface air from the Labrador Sea and the expanded sea ice cap toward south Greenland. There, significant colder conditions (Figure 2e, blue shading) last for as long as four decades (Figure 3), in phase with the oceanic surface cooling. Anomalous cold conditions over the Norse settlements can thus result from locally induced oceanic cooling west of Greenland. Major hemispheric-scale climate fluctuations are therefore not necessary to explain the decadal cold periods reconstructed in this region for the last millennium. As further possible stress factors to the Norse societies, during the simulated cold events the number of days per year with temperatures above the freezing point and of free-snow surface is reduced by between 10 and 20% of the climatology for the region of the Greenland settlements (not shown). In the most extreme case, there are as few as 20 days without snow cover in a year, one of the minimum values detected across all of the simulations. Such reductions imply prolonged periods of unusually or even extremely short harvest seasons. The negative impact on stock supply of these environmental conditions might have posed high risk of large famines to the local population. Norsemen could have then shifted their dietary from terrestrial farming to marine hunting [*Arneborg et al.*, 2012], although it is also suggested that this adaptation might have limited further changes under transforming socioeconomic agents, and might have eventually caused the failure of the settlements in Greenland [*Dugmore et al.*, 2012].

5. Conclusions

This study used last millennium climate simulations to attribute and describe the governing mechanism of decadal-scale cold events in the northern North Atlantic seen in temperature reconstructions of the last millennium. Our results indicate that

1. Decadal cold events in the northern North Atlantic can develop due to internal climate variability alone, although the role of external forcing cannot be excluded, especially concerning the strength of the cold events.
2. The cold events are driven by positive feedbacks within the subpolar North Atlantic linked to weakening and shrinking of the subpolar gyre. The associated shutdown of the Labrador Sea deep convection provides a major negative feedback to the cold events, whose dampening phase is then dominated by substantial weakening of the AMOC. The latter thus occurs as a result of anomalous surface salinity conditions driven by changes of the subpolar gyre strength, and not as a result of a larger freshwater contribution from the Arctic Ocean. Dynamics underlying the cold events described here thus differ from those explaining similar events during the observational period.
3. Living conditions over Greenland notably deteriorate during the cold events due to locally induced anomalous climate situation. A hemispheric-scale reorganization in the climate is not necessary to explain the reconstructed changes within the area. Especially, a series of cold events might have contributed to demise the Norse settlements in Greenland.

Acknowledgments
Data are available from the first author upon request. The MPI-ESM-P simulations were conducted at the German Climate Computing Center (DKRZ). The authors thank Jürgen Bader for comments that helped improving the manuscript. The constructive input of two anonymous referees is gratefully acknowledged.

The Editor thanks two anonymous reviewers for their assistance in evaluating this paper.

References

Arneborg, J., N. Lynnerup, J. Heinemeier, J. Møhl, N. Rud, and Á. E. Sveinbjörnsdóttir (2012), Norse Greenland dietary economy ca. AD 980-ca. AD 1450: Introduction, *J. North Atlantic*, *3*, 1–39.

Born, A., and T. F. Stocker (2014), Two stable equilibria of the Atlantic subpolar gyre, *J. Phys. Oceanogr.*, *44*(1), 246–264.

Braconnot, P., S. P. Harrison, M. Kageyama, P. J. Bartlein, V. Masson-Delmotte, A. Abe-Ouchi, B. Otto-Bliesner, and Y. Zhao (2012), Evaluation of climate models using palaeoclimatic data, *Nat. Clim. Change*, *2*(6), 417–424.
Crowley, T. J., and M. B. Unterman (2012), Technical details concerning development of a 1200-yr proxy index for global volcanism, *Earth Syst. Sci. Data Discuss.*, *5*(1), 1–28, doi:10.5194/essdd-5-1-2012.
Dugmore, A. J., T. H. McGovern, O. Vésteinsson, J. Arneborg, R. Streeter, and C. Keller (2012), Cultural adaptation, compounding vulnerabilities and conjunctures in Norse Greenland, *Proc. Natl. Acad. Sci. U.S.A.*, *109*(10), 3658–3663.
Gelderloos, R., F. Straneo, and C. A. Katsman (2012), Mechanisms behind the temporary shutdown of deep convection in the Labrador Sea: Lessons from the Great Salinity anomaly years 1968–71, *J. Clim.*, *25*(19), 6743–6755, doi:10.1175/JCLI-D-11-00549.1.
Grossmann, I., and P. J. Klotzbach (2009), A review of North Atlantic modes of natural variability and their driving mechanisms, *J. Geophys. Res.*, *114*, D24107, doi:10.1029/2009JD012728.
Hasselmann, K. (1976), Stochastic climate models part I. Theory, *Tellus*, *28*(6), 473–485.
Hátún, H., A. B. Sandø, H. Drange, B. Hansen, and H. Valdimarsson (2005), Influence of the Atlantic subpolar gyre on the thermohaline circulation, *Science*, *309*(5742), 1841–1844.
Hoskins, B. J., and D. J. Karoly (1981), The steady linear response of a spherical atmosphere to thermal and orographic forcing, *J. Atmos. Sci.*, *38*(6), 1179–1196, doi:10.1175/1520-0469(1981)038<1179:TSLROA>2.0.CO;2.
Hunt, B. G. (2009), Natural climatic variability and the Norse settlements in Greenland, *Clim. Change*, *97*(3–4), 389–407, doi:10.1007/s10584-009-9575-5.
Jiang, H., J. Eiríksson, M. Schulz, K. L. Knudsen, and M. S. Seidenkrantz (2005), Evidence for solar forcing of sea-surface temperature on the North Icelandic Shelf during the late Holocene, *Geology*, *33*(1), 73–76, doi:10.1130/G21130.1.
Jungclaus, J. H., et al. (2013), Characteristics of the ocean simulations in the Max Planck Institute Ocean Model (MPIOM) the ocean component of the MPI-Earth system model, *J. Adv. Model. Earth Syst.*, *5*(2), 422–446, doi:10.1002/jame.20023.
Jungclaus, J. H., K. Lohmann, and D. Zanchettin (2014), Enhanced 20th-century heat transfer to the Arctic simulated in the context of climate variations over the last millennium, *Clim. Past*, *10*, 2201–2213, doi:10.5194/cp-10-2201-2014.
Kaufman, D. S., et al. (2009), Recent warming reverses long-term Arctic cooling, *Science*, *325*(5945), 1236–1239.
Knight, J. R., R. J. Allan, C. K. Folland, M. Vellinga, and M. E. Mann (2005), A signature of persistent natural thermohaline circulation cycles in observed climate, *Geophys. Res. Lett.*, *32*, L20708, doi:10.1029/2005GL024233.
Kuijpers, A., N. Mikkelsen, S. Ribeiro, and M. S. Seidenkrantz (2014), Impact of medieval fjord hydrography and climate on the western and eastern settlements in Norse Greenland, *J. North Atlantic*, *6*, 1–13, doi:10.3721/037.002.sp603.
Langehaug, H. R., I. Medhaug, T. Eldevik, and O. H. Otterå (2012), Arctic/Atlantic exchanges via the subpolar gyre, *J. Clim.*, *25*(7), 2421–2439.
Marshall, J., Y. Kushnir, D. Battisti, P. Chang, A. Czaja, R. Dickson, J. Hurrell, M. McCartney, R. Saravanan, and M. Visbeck (2001), North Atlantic climate variability: Phenomena, impacts and mechanisms, *Int. J. Climatol.*, *21*, 1863–1898, doi:10.1002/joc.693.
Massé, G., S. J. Rowland, M.-A. Sicre, J. Jacob, and S. T. Belt (2008), Abrupt climate changes for Iceland during the last millennium: Evidence from high resolution sea ice reconstructions, *Earth Planet. Sci. Lett.*, *269*(3), 565–569, doi:10.1016/j.epsl.2008.03.017.
Miller, G. H., et al. (2012), Abrupt onset of the Little Ice Age triggered by volcanism and sustained by sea-ice/ocean feedbacks. *Geophys. Res. Lett.*, *39*, L02708, doi:10.1029/2011GL050168.
Moffa-Sánchez, P., A. Born, I. R. Hall, D. J. Thornalley, and S. Barker (2014a), Solar forcing of North Atlantic surface temperature and salinity over the past millennium, *Nat. Geosci.*, doi:10.1038/ngeo2094.
Moffa-Sánchez, P., I. R. Hall, S. Barker, D. J. Thornalley, and I. Yashayaev (2014b), Surface changes in the eastern Labrador Sea around the onset of the Little Ice Age, *Paleoceanography*, *29*, 160–175, doi:10.1002/2013PA002523.
Ogilvie, A. E., L. K. Barlow, and A. E. Jennings (2000), North Atlantic climate c. AD 1000: Millennial reflections on the Viking discoveries of Iceland, Greenland and North America, *Weather*, *55*(2), 34–45, doi:10.1002/j.1477-8696.2000.tb04028.x.
Patterson, W. P., K. A. Dietrich, C. Holmden, and J. T. Andrews (2010), Two millennia of North Atlantic seasonality and implications for Norse colonies, *Proc. Natl. Acad. Sci. U.S.A.*, *107*(12), 5306–5310, doi:10.1073/pnas.0902522107.
Pongratz, J., C. Reick, T. Raddatz, and M. Claussen (2008), A reconstruction of global agricultural areas and land cover for the last millennium, *Global Biogeochem. Cycles*, *22*, GB3018, doi:10.1029/2007GB003153.
Ran, L., H. Jiang, K. L. Knudsen, and J. Eiríksson (2011), Diatom-based reconstruction of palaeoceanographic changes on the North Icelandic shelf during the last millennium, *Palaeogeogr. Palaeoclimatol. Palaeoecol.*, *302*(1), 109–119, doi:10.1016/j.palaeo.2010.02.001.
Schmidt, G. A., et al. (2011), Climate forcing reconstructions for use in PMIP simulations of the last millennium (v1. 0), *Geosci. Model Dev.*, *4*(1), doi:10.5194/gmd-4-33-2011.
Sicre, M.-A., et al. (2011), Sea surface temperature variability in the subpolar Atlantic over the last two millennia, *Paleoceanography*, *26*, PA4218, doi:10.1029/2011PA002169.
Stevens, B., et al. (2013), Atmospheric component of the MPI-M Earth System Model: ECHAM6, *J. Adv. Model. Earth Syst.*, *5*(2), 146–172, doi:10.1002/jame.20015.
Vieira, L. E. A., S. K. Solanki, N. A. Krivova, and I. Usoskin (2011), Evolution of the solar irradiance during the Holocene, *A & A, 531(A6)*, 20, doi:10.1051/0004-6361/201015843.
Visbeck, M., E. P. Chassignet, R. G. Curry, T. L. Delworth, R. R. Dickson, and G. Krahmann (2003), The ocean's response to North Atlantic Oscillation variability, in *The North Atlantic Oscillation: Climatic Significance and Environmental Impact*, edited by J. W. Hurrell et al., pp. 113–145, AGU, Washington, D. C., doi:10.1029/134GM06.
Yashayaev, I. (2007), Hydrographic changes in the Labrador Sea, 1960–2005, *Prog. Oceanogr.*, *73*(3), 242–276.
Zanchettin, D., C. Timmreck, H.-F. Graf, A. Rubino, S. Lorenz, K. Lohmann, K. Krüger, and J. H. Jungclaus (2012), Bi-decadal variability excited in the coupled ocean–atmosphere system by strong tropical volcanic eruptions, *Clim. Dyn.*, *39*(1–2), 419–444, doi:10.1007/s00382-011-1167-1.